

# Corrosion Behavior of Electromagnetic Shielding Coating under the Interaction of Steady Magnetic Field with Corrosion Medium

*Shuting Fan, Minna Yang, Lin Lu<sup>\*</sup>, Zebang He*

Corrosion and Protection Center, University of Science and Technology Beijing, Beijing 100083, China

\*E-mail: [lulin315@126.com](mailto:lulin315@126.com)

*Received: 28 April 2017 / Accepted: 24 July 2017 / Published: 12 September 2017*

---

Electrochemical impedance spectroscopy was conducted to analyze the influence of coating properties on the corrosion behavior of electromagnetic shielding coating (EMSC) in a 3.5 wt.% NaCl solution under a 0.1 T steady magnetic field (MF). The results showed that the coating fillers and the acting time in the MF were the key factors affecting the corrosion behavior of the EMSC. The MF had a homogenizing effect on magnetic fillers in the coating, which could improve the corrosion resistance of the coating, but it could not play the same role in a coating with non-magnetic fillers. Moreover, the strength of the homogenizing effect depended on the acting time in the MF. The penetration of the solution into the topcoats of a double-layer EMSC was found to provide more time for the movement of the filler in the primers, compared with the time taken by a single layer system. Therefore, the EMSC primer in the double-layer system presented better corrosion resistance, which was manifested by the EIS results.

---

**Keywords:** magnetic filler; magnetic field; homogenizing effect; electromagnetic shielding coating; electrochemical impedance spectroscopy

## 1. INTRODUCTION

Electromagnetic radiation interference directly affects the operation of electronic equipment in various industries, poses serious threats to information security, and can bring about immeasurable damage to the health of mankind [1]. As the main components of electromagnetic shielding, metal shells and electromagnetic shielding coatings (EMSC) are utilized widely to improve the electromagnetic compatibility of electronic systems and electronic equipment. Current research into EMSC mainly concentrates on how to improve their shielding performance. As discussed in Refs [2-

5], it is possible to improve electromagnetic shielding effectiveness by adding an alloying element, improving the ability for amorphous forming, refining the particles, coating the surface of the alloy powder and forming a double-layer coating structure. Wu et al. [6] found that when the amount of titanate coupling agent used was 1.25% (mass fraction) of the nickel filler, the homogenizing effect of the coating became better. The coating had a 35 dB shielding effectiveness in the range considered, 9 kHz~1.3 GHz. Feng Tao et al. [7] studied the effect of a magnetic field on the microstructure of thermosetting composites. The results showed that the orientation of the filler in the coating increases under a magnetic field. In addition, the use of a sheet-like filler and the selection of an appropriate coupling agent could improve electromagnetic shielding effectiveness of the coating[8-15].

Comparatively, few papers have focused on the environmental adaptability of the EMSC under the interaction of a magnetic field with a natural environment. In fact, the shielding effects are related to the corrosion resistance of the shielding materials. Xuan et al. [16] found that after 96 h of a continuous salt spray test, the shielding effect of a Ni-P-La alloy EMSC was almost unchanged. Szewieczek et al. [17] investigated the effect of electrochemical corrosion on magnetic properties and found that the saturation magnetization of a  $\text{Fe}_{73.5}\text{Si}_{13.5}\text{B}_9\text{Nb}_9\text{Cu}_1$  alloy decreased after 15 d of exposure to a 0.5 M  $\text{Na}_2\text{SO}_4$  solution at a temperature of 20°C. Therefore, it is necessary to first explore the corrosion behavior of an EMSC under the service conditions, which is a prerequisite for further improvement of the shielding effect.

EMSCs used in marine environment are subject to attack by severe environmental conditions and by the magnetic field (MF) generated by electronic instruments. Thus, the effect of a MF on the corrosion behavior of the coating is a key problem to solve. Our research group has found that a magnetic field can accelerate the vertical penetration of the electrolyte into the coating system and the diffusion process at the interface of the coating and the substrate [18]. However, the specific effect of the MF on the distribution of the fillers, and its corresponding influence on the corrosion resistance of the coating system needs further investigation.

In this paper, the corrosion behavior of coatings with different fillers were studied under a magnetic field. The mechanism of the action of the MF on the corrosion behavior is discussed in detail, and the magnetism of the fillers and the acting time in the MF are emphasized as the most important factors.

## 2. EXPERIMENTAL

### 2.1 Materials

Q235 mild carbon steel was used as the metal substrate. A two component acrylic polyurethane liquid was supplied by Dow Corning Corporation. Nano-scale  $\text{TiO}_2$  was purchased from Nano Applied Research Center of Nanjing University of Technology. The Ni-based electromagnetic shielding coating (Ni-based EMSC) was purchased from Advanced Technology & Materials Co., Ltd. Other solvents and analytic reagents were purchased from Sinopharm Corporation and used as received.

## 2.2 Preparation of coatings

The carbon steel was cut to a size of 75 mm × 50 mm × 1 mm, sequentially polished with 240 grit abrasive paper to remove mill scale and then cleaned with acetone in an ultrasonic bath.

Three types of single-layer acrylic polyurethane coatings were studied in this research, including a Ni-based EMSC, acrylic polyurethane varnish coating and an acrylic polyurethane coating filled with titanium dioxide. All of them were coated on the substrate by brushing, cured at 50°C for 2 h and then subsequently cured at room temperature for a week. The thickness of coatings was ~80 μm. The electromagnetic shielding effectiveness (SE) of the nickel-based coating was measured in the range of 0~3000 MHz by the flange coaxial method, and it was shown that the SE of the coating with nickel fillers was ~50 dB.

A double-layer coating system was also investigated, in which an acrylic polyurethane varnish coating served as a topcoat, and a Ni-based EMSC (50 μm) served as a primers. The thicknesses of coatings were ~80 μm.

## 2.3 EIS measurements

Electrochemical impedance spectroscopy (EIS) was performed in a 3.5 wt.% NaCl solution using a PARSTAT 2273 electrochemical station (Princeton, USA). A Faraday cage was used during all electrochemical measurements. A three-electrode system was used, consisting of the coated panel as the working electrode (with an exposed area of 1 cm<sup>2</sup>), a saturated calomel electrode (SCE) as the reference electrode and a platinum electrode as the counter electrode (CE). The working electrode (WE) was first immersed in test electrolyte for at least 20 min to stabilise the electrode before the coating potential ( $E_{\text{coat}}$ ) was recorded with an open circuit. The measurements were carried out at ambient temperature (~25°C). A homemade magnetic field generator was used to impose a stable 0.1 T MF on the coating system, a sketch of which is shown in Fig. 1. The generator mainly consists of a DC power supply, coil and magnetic poles.

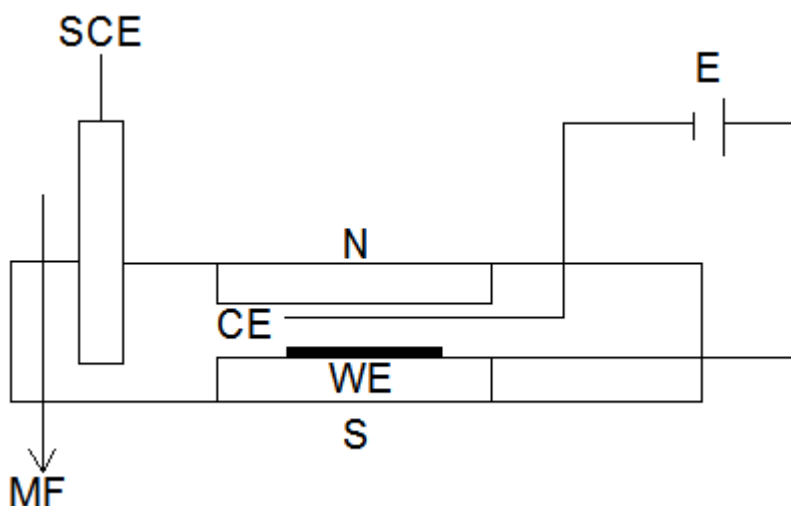


**Figure 1.** Homemade magnetic field generating device.

### 3. RESULTS AND DISCUSSION

#### 3.1 Effect of different fillers on the corrosion behavior of the coatings systems under a magnetic field

##### 3.1.1 EIS characteristics of the coatings in 3.5 wt.% NaCl under a 0.1 T MF

EIS results for the Ni-based EMSC were obtained after different periods of immersion, as shown in Fig. 2. Comparing with the spectra acquired for the original state (0 h), it can be seen that after one hour the diameter of the capacitive arc appears to increase in the Nyquist plots, and the  $|Z|_{0.01 \text{ Hz}}$  value increases by an order of magnitude in Bode plots. From then on, the value of  $|Z|_{0.01 \text{ Hz}}$  has maintained at  $\sim 8 \times 10^5 \Omega \cdot \text{cm}^2$  in the Bode plots until the 72<sup>th</sup> hour. Finally, the  $|Z|_{0.01 \text{ Hz}}$  values decreases to  $\sim 2 \times 10^3 \Omega \cdot \text{cm}^2$  after 96 hours of immersion, which means that at this point the coating has failed.

Comparatively, for the acrylic polyurethane coating, the  $|Z|_{0.01 \text{ Hz}}$  values decreases by an order of magnitude in the Bode plots after only one hour of immersion, as shown in Fig. 3. The diameter of the capacitive arc in Nyquist plots decreases constantly with immersion time, and the corresponding  $|Z|_{0.01 \text{ Hz}}$  values decreases by four orders of magnitude in the Bode plots after 8 hours of immersion. The Nyquist plot transforms from one large capacitive arc into two capacitive arcs, which implies a failure of the coating. After immersing for 24 hours, the diameter of the capacitive arc significantly reduces in the Nyquist plots, meaning that the coating has completely failed.

Figure 4 shows EIS spectra of the coating filled with  $\text{TiO}_2$ . The same trend in the spectra is observed, however, the rate of decrease in the  $|Z|_{0.01 \text{ Hz}}$  value slows down significantly. For the varnish coating, after only one day the  $|Z|_{0.01 \text{ Hz}}$  value reaches  $10^5 \Omega \cdot \text{cm}^2$ . In comparison, the  $|Z|_{0.01 \text{ Hz}}$  value of the coating filled with  $\text{TiO}_2$  does not reach  $10^5 \Omega \cdot \text{cm}^2$  until the seventh day. As discussed in Refs [19], the MF can accelerate penetration of the solution, that is, the movement of anions perpendicular to the direction of MF ( $v_{\perp}$ ) would be driven by the Lorentz Force  $F$ , and the movement parallel to the direction of MF would be affected by another Lorentz Force generated by  $v_{\perp}$  cutting the magnetic induction lines. Based on the above analysis, it can be deduced that the filler effectively delays the electrolyte diffusion penetration even when the accelerating effect of the MF works on the coating system.

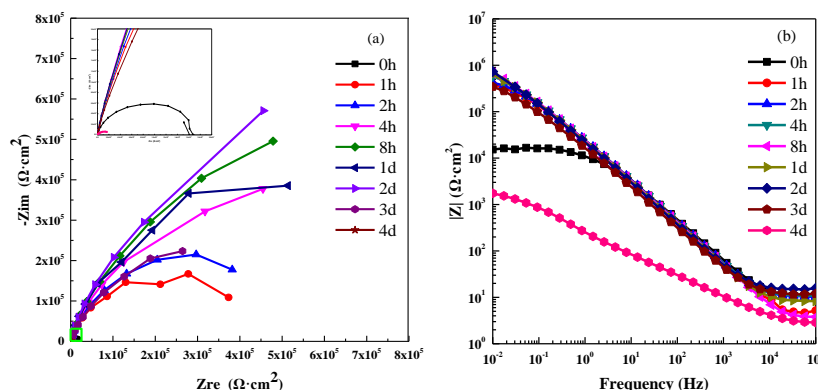


**Figure 2.** Impedance spectra of the Ni-based EMSC in 3.5 wt.% NaCl solution under the magnetic field; (a) Nyquist plots, (b) Bode Z plots.

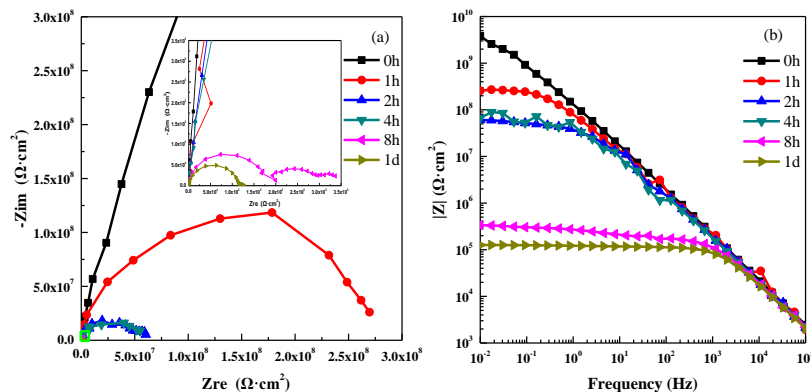


**Figure 3.** Impedance spectra of the acrylic polyurethane coating in 3.5 wt.% NaCl solution under the magnetic field; (a) Nyquist plots, (b) Bode Z plots.

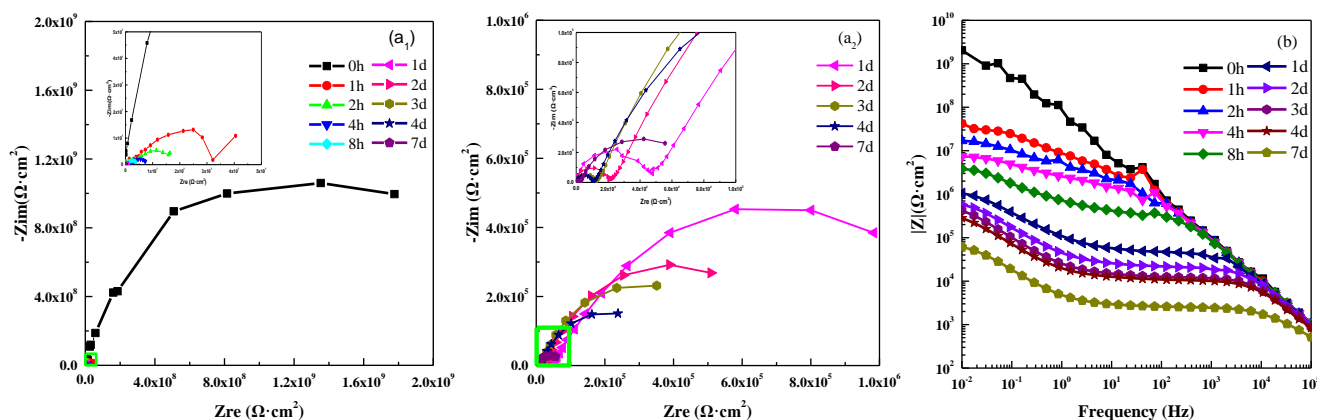


**Figure 4.** Impedance spectra of the acrylic polyurethane coating filled with TiO<sub>2</sub> in 3.5 wt.% NaCl solution under the magnetic field; (a<sub>1</sub>) (a<sub>2</sub>) Nyquist plots, (b) Bode Z plots.

### 3.1.2 Different effects of fillers on the corrosion behavior of coatings under 0.1 T MF

It can be seen from Fig. 5 that, if the filler is non-magnetic, the  $|Z|_{0.01 \text{ Hz}}$  values of the coating decrease completely during the immersion period, similar to that presented by the varnish coating. Since TiO<sub>2</sub> particles fill the large pores in the coating, the corrosion resistance of the coating is increased [20-22], and thus the rate of decrease of the  $|Z|_{0.01 \text{ Hz}}$  values is much slower than that of varnish coating. In addition, the accelerating effect on the electrolyte resulting from the MF is reduced due to the addition of fillers. That is to say, the penetration process slows down.

If the filler is nickel particles, the  $|Z|_{0.01 \text{ Hz}}$  value of the coating exhibits an increasing trend in the first few days of immersion and then decreases, which is different from the other two coatings. This may be attributed to the magnetism of the filler, which can be magnetized along the magnetic direction in the MF. Therefore, each filler particle can be seen as a small magnet with a north pole and a south pole, and adjacent filler particles are subject to a magnetic force generated by other particles. In order for the system to finally reach a force equilibrium state, the filler is redistributed in the resin and

the coating structure becomes more uniform, during which like poles repel and unlike poles attract each other.[23-25]. Finally, the rearrangement of the particles makes the permeation path of the electrolyte more roundabout (Fig. 6) than before, and the diffusion process into the coating needs much more time under the MF. As a result, it is difficult for the solution to penetrate through the coating and all corrosion processes are consequently slowed down, as shown in Fig. 2.

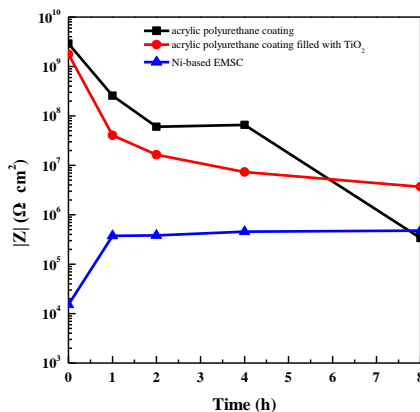


**Figure 5.** The  $|Z|_{0.01 \text{ Hz}}$  value for three kinds of coating within 8 hours.

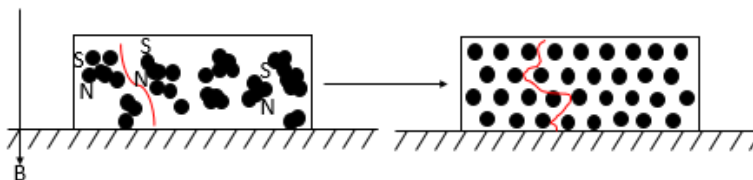


**Figure 6.** Schematic diagram of the distribution of the Ni filler under a magnetic field.

### 3.2 The effect of the double-layer coating system on the electrochemical behavior of coatings under a MF

#### 3.2.1 Corrosion processes involved in the double layer EMSC

Figure 7 shows EIS spectra of a double-layer coating system for different immersion periods. During the first 12 hours, the coating shows a strong barrier effect by presenting only one large capacitive arc with a minimal decrease in its diameter, and the  $|Z|_{0.01 \text{ Hz}}$  value of the coating remains at approximately  $10^9 \text{ } \Omega \cdot \text{cm}^2$  in the Bode plots. After 24 hours of immersion, the diameter of the capacitive arc decreases significantly in the Nyquist plots, and the  $|Z|_{0.01 \text{ Hz}}$  value decreases to  $10^4 \sim 10^5 \text{ } \Omega \cdot \text{cm}^2$  in the Bode plots. This is the same magnitude as that observed for the varnish coating (Fig. 3), which indicates that the solution has penetrated into the topcoat and reached the interface of the two layers. From the second day to the third day, the diameter of the capacitive arc slightly decreases in the Nyquist plots, which may be attributed to the diffusion of the solution into the primer. On the fifth day of immersion, the diameter of the capacitive arc slightly increases in the Nyquist plots, indicating that

at this time the magnetic field still has homogenizing effect on the filler in the primer. Then, the diameter of the capacitive arc shows almost no change in the Nyquist plots, and the  $|Z|_{0.01 \text{ Hz}}$  values remains at the same level in the Bode plots until the 11<sup>th</sup> day.

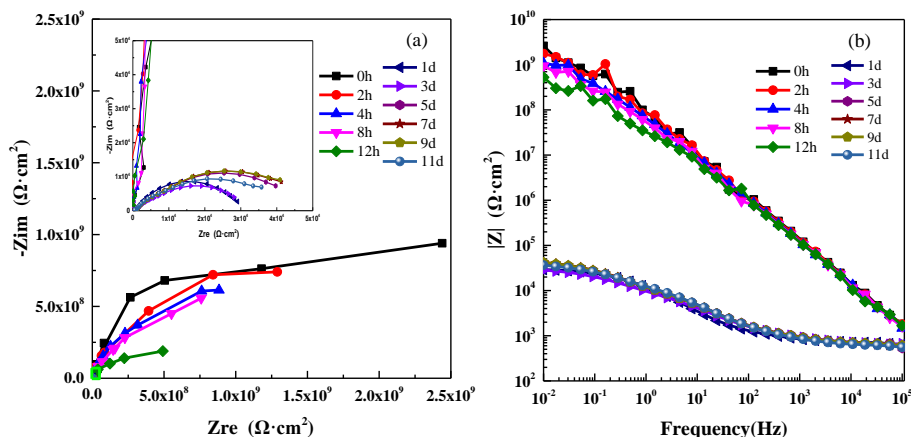


**Figure 7.** Impedance spectra of the double-layer EMSC (80  $\mu\text{m}$ ) in 3.5 wt.% NaCl solution under the magnetic field; (a) Nyquist plots, (b) Bode Z plots.

The EIS data were further fitted with three different equivalent electrical circuits (EECs), as shown in Fig. 8, and the fitting results are listed in Table 1. In the equivalent circuit,  $R_s$  represents the solution resistance,  $Q_{c1}$  represents the capacitance of the acrylic polyurethane coating,  $R_{c1}$  represents the resistance of the acrylic polyurethane coating,  $Q_{c2}$  represents the capacitance of the Ni-based EMSC,  $R_{c2}$  represents the resistance of the Ni-based EMSC,  $Q_{Ni}$  represents the double layer capacitance of the Ni filler and resin interface and  $R_{Ni}$  represents the charge transfer resistance during the corrosion process. Correspondingly, the corrosion process of the double layer coating system can be divided into three stages during the whole test period.

In the first stage, the two-layer system can be seen as one entity during the first 12 hours of immersion, the EEC of which is shown in Fig. 8a [26-28]. At this stage, the top coating is immersed in the electrolyte, which can be verified by an increase in  $Q_{c1}$  and a decrease in  $R_{c1}$ .

In the second stage, after 1 d, the solution reaches the interface between the topcoat and the primer. At this point, the corrosion reaction can occur at the interface between the nickel filler and the resin. These processes could be simulated by the EEC shown in Fig. 8b [29-31]. Similarly, Liu et al. [29] studied the corrosion behaviour of a zinc-rich primer/chlorinated rubber top coating double-layered system. They found that this EEC (Fig 8b) could be used to describe the electrochemical corrosion process at the metal-filler interface [30,31]. Based on the above, it could be proven that at this time, an electrochemical reaction occurs at the interface of the nickel filler and the electrolyte.

In the third stage, the top coating has almost lost its protective effect against the electrolyte, and only has a residual resistance of several hundred Ohms. That is, the solution can penetrate the topcoat and arrive at the primer without any barrier. However, the solution cannot penetrate the primer easily. Verifying this, the primer,  $|Z|_{0.01 \text{ Hz}}$  values remained unchanged at  $2 \times 10^4$  Ohms in the Bode plots during the following test days.

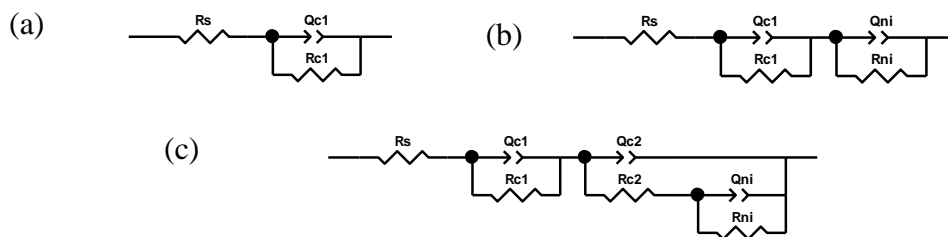


**Figure 8.** Electrical equivalent circuits used for fitting the EIS spectra.

**Table 1.** Electrochemical parameters fitted from EIS results for coatings in the immersion tests.

Time	EEC	Q <sub>c1</sub> (F/cm <sup>2</sup> )	R <sub>c1</sub> (Ω·cm <sup>2</sup> )	Q <sub>c2</sub> (F/cm <sup>2</sup> )	R <sub>c2</sub> (Ω·cm <sup>2</sup> )
0h	R(QR)	1.753E-9	1.434E9	---	---
2h	R(QR)	1.841E-9	8.425E8	---	---
4h	R(QR)	2.672E-9	7.23E8	---	---
8h	R(QR)	2.786E-9	2.727E8	---	---
12h	R(QR)	3.749E-9	1.135E8	---	---
1d	R(QR)(QR)	2.022E-5	3.02E4	---	---
3d	R(QR)(Q(R(QR)))	2.929E-9	667.1	2.941E-5	2.597E4
5d	R(QR)(Q(R(QR)))	2.5E-9	501.5	2.098E-5	2.832E4
7d	R(QR)(Q(R(QR)))	3.587E-9	648	1.956E-5	2.774E4
9d	R(QR)(Q(R(QR)))	1.761E-9	654.2	2.019E-5	2.579E4
11d	R(QR)(Q(R(QR)))	4.804E-8	613.9	1.741E-5	2.412E4

### 3.2.2 Effect of acting time of in the MF on the electrochemical behavior of the coatings

Based on the above results, it could be deduced that a primer with a thickness of 50 μm still maintained good corrosion resistance after 10 d of immersion, when the solution arrived at the interface of the top layer and the primer. However, the single layer EMSC with a thickness of 80 μm was penetrated in four days. The difference between the corrosion behaviors of these two EMSC systems could be assigned to the acting time in the MF, which might influence the various structural features of the EMSC.

For convenience of the analysis, the nickel particles in the EMSC can be approximated as ellipsoids, with  $x_c$  as the long axis and  $x_a$  as the short axis. According to the literature [32], the time required for magnetic particles to rotate from the initial state  $\theta_0$  to the equilibrium position  $\theta$  under a magnetic field can be expressed by the following two formulas:

$$\theta = \tan^{-1}(\tan\theta_0 \exp(\alpha t)) \tag{1}$$



$$t = \frac{4\eta f(k)}{u_0(x_a - x_c)H^2} \ln\left(\frac{\tan\theta^*}{\tan\theta_0}\right) \quad (2)$$

Where  $\alpha = \frac{u_0 H^2}{4\eta f(k)}(x_a - x_c)$ ,  $\eta$  is the kinetic viscosity of the system,  $x_a$  and  $x_c$  are the axial susceptibilities,  $H$  is the MF intensity,  $u_0$  is the vacuum permeability, and  $f(k)$  is a function of the aspect ratio. The rotation of the particles is completed when  $\theta = \theta^*$ . The above equation proves that the magnetic particles do take some time to move around. The rotation time is inversely proportional to the square of the MF intensity and is directly proportional to the length of the particles.

Compared with the double-layer system, the filler in the single-layer EMSC had less time for movement before the electrolyte penetrated through the coating, because it underwent diffusion of electrolyte and the rearrangement of the nickel particles at same time. To some extent, the diffusion process counteracted the homogenization effect of the MF on the fillers. Comparatively, the process of electrolyte penetration into the top-coat of the double-layer EMSC provided a much longer time to spin and move, which made the primer a more homogeneous structure and enhanced its corrosion protection. Therefore, the acting time in the MF played an important role on the improvement of corrosion resistance for the EMSCs.

#### 4. CONCLUSIONS

The electrochemical behaviors of coating systems with different fillers and the corrosion processes related to a double-layer coating system were studied in a 3.5 wt.% NaCl solution under a 0.1 T MF. The following conclusions can be drawn.

(1) When a 0.1 T MF is imposed, a single-layer EMSC presents an enhanced barrier effect to electrolyte diffusion, and the  $|Z|_{0.01 \text{ Hz}}$  is sharply increased by more than one order of magnitude.

(2) The effect of the MF on the distribution of the filler in coatings depended on the magnetism of the filler. It was shown that nickel particles could be rearranged in the coating by imposing a 0.1 T MF. However, a non-magnetic filler,  $\text{TiO}_2$ , did not show any indication of this effect.

(3) Compared to the single-layer EMSC, the EMSC primer in the double-layer system presented better corrosion resistance, which could be attributed to the longer acting time of the MF.

#### ACKNOWLEDGEMENTS

This work was supported by the National Natural Science Foundation of China (No. U1560104), the National Key Research and Development Program of China (No. 51133009), the National Basic Research Program of China (No. 2014CB643300) and the National Environmental Corrosion Platform (NECP).

#### References

1. N. E. Kamchi, B. Belaabed and J. L. Wojkiewicz, *J. Appl. Polym. Sci.*, 127 (2013) 4426
2. L. Zhou, Y. Z. Yang and P. J. Tao, *Trans. Mater. Heat Treat.*, 18 (2012) 0024
3. C. L. Zhu, Q. Wang and X. M. Wang, *Rare Met. Mater. Eng.*, S4 (2008) 773
4. Z. Q. Hu, H. F. Zhang, *Acta Metall. Sin.*, 11 (2010) 1391
5. J. E. May, P. A. P. Nascente, S. E. Kuri, *Corros. Sci.*, 48 (2006) 1721

6. H. Wu, J. Z. Chen and M. J. Tu, *J. Funct. Mater.*, 31 (2000) 262
7. F. Chao, G. Liang, W. Kong, Z. Zhang and J. Wang, *Polym. Bull.*, 60 (2008) 132.
8. C Wang, Y Shen and X Wang, *Mater. Sci. Semicond. Process.*, 16 (2013) 77
9. C Wang, Y Shen, X Wang and H Zhang, *Mater. Sci. Semicond. Process.*, 16 (2013) 77.
10. M. Yu, Q. Xu and X. Pang, *Aerospace Mater. Technol.*, 42 (2012) 12
11. M. Jalali, S Dauterstedt and A Michaud, *Compos. Part B:Eng.*, 42 (2011) 1420
12. T. D. Prichard, B. D. Vogt, *Polym. Eng. Sci.*, 53 (2013) 69
13. J. Pang, Q Li, W Wang and X Xu, *Surf. Coat. Technol.*, 205 (2011) 4237
14. J. Pang, Q Li and W Wang, *Powder Technol.*, 226 (2012) 246
15. H Wu, J. Z. Chen and M. J. Tu. *J. Funct. Mater.*, 31 (2000) 262
16. T. Xuan, G. Yang and L. Yang, *J. Rare Earths*, 24 (2006) 389
17. D. Szewieczek, A Baron, *J. Mater. Process. Technol.*, 164-165 (2005) 940
18. M. Yang, L. Lu, J. Gao and X. Li, *J. Funct. Mater.*, 24 (2015) 24088
19. M. Ghabashy. *Anti-corrosion Methods Mater.*, 35 (1988) 12
20. Y. C. Ching, N Syamimie, *J. Nanomaterials*, 2013 (2013) 17
21. P. Donkers, H. Huinink and S. Erich, *Prog. Org. Coat.*, 76 (2013) 60
22. V. Spagnol, E. Sutter, C. Chouvy and H. Cacheta, *Electrochim. Acta*, 54 (2009) 1228
23. M. Ghabashy, G. Sedahmed and I. Mansour, *British Corrosion Journal*, 17 (1982) 36
24. J. Hu, C. Dong, X. Li and K Xiao. *J. Mater. Sci. Technol.*, 2010, 26 (4) 355-361
25. K. Busch, M. Buxdh and D. Parker, *Corros.*, 42 (1986) 211
26. C. Chen, S. Qiu, S. Qin, G. Yan, H. Zhao and L. Wang, *Int. J. Electrochem. Sci.*, 12 (2017) 3417
27. X.P Liu, T.L Zheng and J.P. Xiong, *Int. J. Electrochem. Sci.*, 8 (2013) 11588
28. J. Li, L. Ecco, M. Fedel, V. Ermini, G. Delmas and J. Pan, *Prog. Org. Coat.*, 87 (2015) 179
29. J.T. Zhang, J.M. Hu, J.Q. Zhang and C.N. Cao, *Prog. Org. Coat.*, 49 (2004) 293
30. X. Liu, J. Xiong, Y. Lv and Y. Zuo, *Prog. Org. Coat.*, 64 (2009) 497
31. F. Kong, J. Zhao, *Corros. Prot.*, 33 (2012) 489
32. B. Zhang, Z. Ren and H. Wang, *Acta Metall. Sin.*, 40 (2004) 604